Application of the weight function method on a high incidence research aircraft model

N. Anton

R. M. Botez
ruxandra@gpa.etsmtl.ca

D. Popescu

École de technologie supérieure
Laboratory of Research in Active Controls, Aeroservoelasticity and Avionics
Montréal
Québec, Canada

ABSTRACT

This paper assesses the application of a new method for system stability analysis, the weight functions method, to the longitudinal and lateral motions of a High Incidence Research Aircraft Model. The method consists of finding the number of weight functions that is equal to the number of differential equations required for system modelling. The aircraft's stability is determined from the sign of the total weight function; which should be negative for a stable model. The Aero-Data Model In Research Environment (ADMIRE) simulation, developed by the Swedish Defence Research Agency, was used for the aerodynamic aircraft modelling, with the following configurations: Mach number = 0·25, altitude = 500m, angle-of-attack [–10 to 30]°, elevon deflection angle [–30 to 30]°, canard deflection [0° and 25°] and rudder deflection angles [–30° and 30°]. These flight configurations were selected because they are among the flight conditions for Cat. II Pilot Induced Oscillation (PIO) criteria validation, performed on the FOI aircraft model presented in the PIO Handbook by the Group for Aeronautical Research and Technology in Europe, *Flight Mechanics/Action Group 12*. This aircraft model has a known instability for longitudinal and lateral motions and so a control law was introduced to stabilise its flight.

Paper No. 3921. Manuscript received 25 October 2012, revised version received 2 April 2013, accepted 12 April 2013.

NOMENCLATURE

b wingspan
C mean aerodynamic chord
C_l roll moment coefficient
C_m pitch moment coefficient
C_n yaw moment coefficient
C_D drag coefficient
C_L lift coefficient
C_T tangential force coefficient
C_y side force coefficient
g acceleration due to gravity
H altitude
I_x x body moment of inertia
I_{xy} x-y body axis product of inertia
I_z z body axis product of inertia
I_y y body axis moment of inertia
I_β rolling moment due to the sideslip angle derivative
$I_{\alpha\beta}$ rolling moment due to the roll rate derivative and alpha derivative
$l_{\delta a}$ rolling moment due to the aileron derivative and alpha derivative
$l_{\alpha\delta a}$ rolling moment due to the aileron derivative
$l_{\delta a}$ rolling moment due to the rudder derivative
l_r rolling moment due to the yaw rate derivative
l_p rolling moment due to the roll rate derivative
m aircraft total mass
M Mach number
n_β yawing moment due to the sideslip angle derivative
$n_{\alpha p}$ yawing moment due to the roll rate derivative and alpha derivative
$n_{\alpha\delta a}$ yawing moment due to the aileron derivative and alpha derivative
$n_{\delta a}$ yawing moment due to the aileron derivative
$n_{\delta r}$ yawing moment due to the rudder derivative
n_r yawing moment due to the yaw rate derivative
n_p yawing moment due to the roll rate derivative
p roll angular rate
q pitch angular rate
$\tilde{q}$ dynamic pressure
r yaw angular rate
S wing surface
T traction
x_{eng} x-position of the engine's centre of gravity
x_{cg} x-position of the centre of gravity
y_β side force due to the sideslip angle derivative
$y_{\delta a}$ side force due to the aileron derivative
$y_{\delta r}$ side force due to the rudder derivative
y_r side force due to the yaw rate derivative
y_p side force due to the roll rate derivative
w weight function

https://doi.org/10.1017/S0001924000008575 Published online by Cambridge University Press

W total weight function
α angle-of-attack
β angle of sideslip
δ_a aileron deflection
δ_c canard deflection
δ_e elevator deflection
δ_r rudder deflection
ϕ roll angle
Φ bank angle
θ pitch angle
ψ heading angle

ABBREVIATIONS AND ACRONYMS

ADMIRE	Aero-Data Model in Research Environment
AG	Action Group
DLR	Deutsches Zentrum für Luft-und Raumfahrt e.V.
GARTEUR	Group for Aeronautical Research and Technology in EURope
FM	Flight Mechanics
FOI	Swedish Defence Research Agency
HIRM	High Incidence Research Aircraft Model
LARCASE	Laboratory of Research in Active Controls, Aeroservoelasticity and Avionics
PIO	Pilot-Involved (Pilot-Induced) (Pilot-In-the-loop) Oscillations
SAAB	Saab AB

1.0 INTRODUCTION

The Weight Function Method (WFM) has been applied in various engineering fields. For example, it has been used to determine stress factors for crack problems. The WFM was applied by Yoichi *et al*[1] to solve two- and three-dimensional crack problems and to calculate stress intensity factors for arbitrary loading conditions. Their application has been generalised to calculate the response analysis of structures and to solve two-dimensional elasticity and plate bending problems. The weight function method was found to be useful for analysing structures subjected to a variety of loading conditions because the responses expressed in terms of displacements and stresses may be calculated by integrating the inner product of a universal weight function and a load vector. The stress intensity factor for a patched crack within an infinite plate was successfully numerically validated using the WFM[2].

Paris *et al*[3] presented an alternate method of Bueckner and Rice for the deviation of a two-dimensional weight function to eliminate crack tip stress intensity factors. A generalised weight function method was developed[4], based on Betti's reciprocal theorem application to the equivalent cracks problem involving mixed boundary conditions. Fett[5] contributed an analytical solution for determining stress distribution using a weight function based on the Boundary Collocation Method. Schneider *et al*[6] used a closed-form weight function formula to calculate the stress intensity factor of an edge crack for an elastic disc. A three-dimensional linear elastic fracture mechanics (LEFM) problem was also solved using the WFM[7].

https://doi.org/10.1017/S0001924000008575 Published online by Cambridge University Press

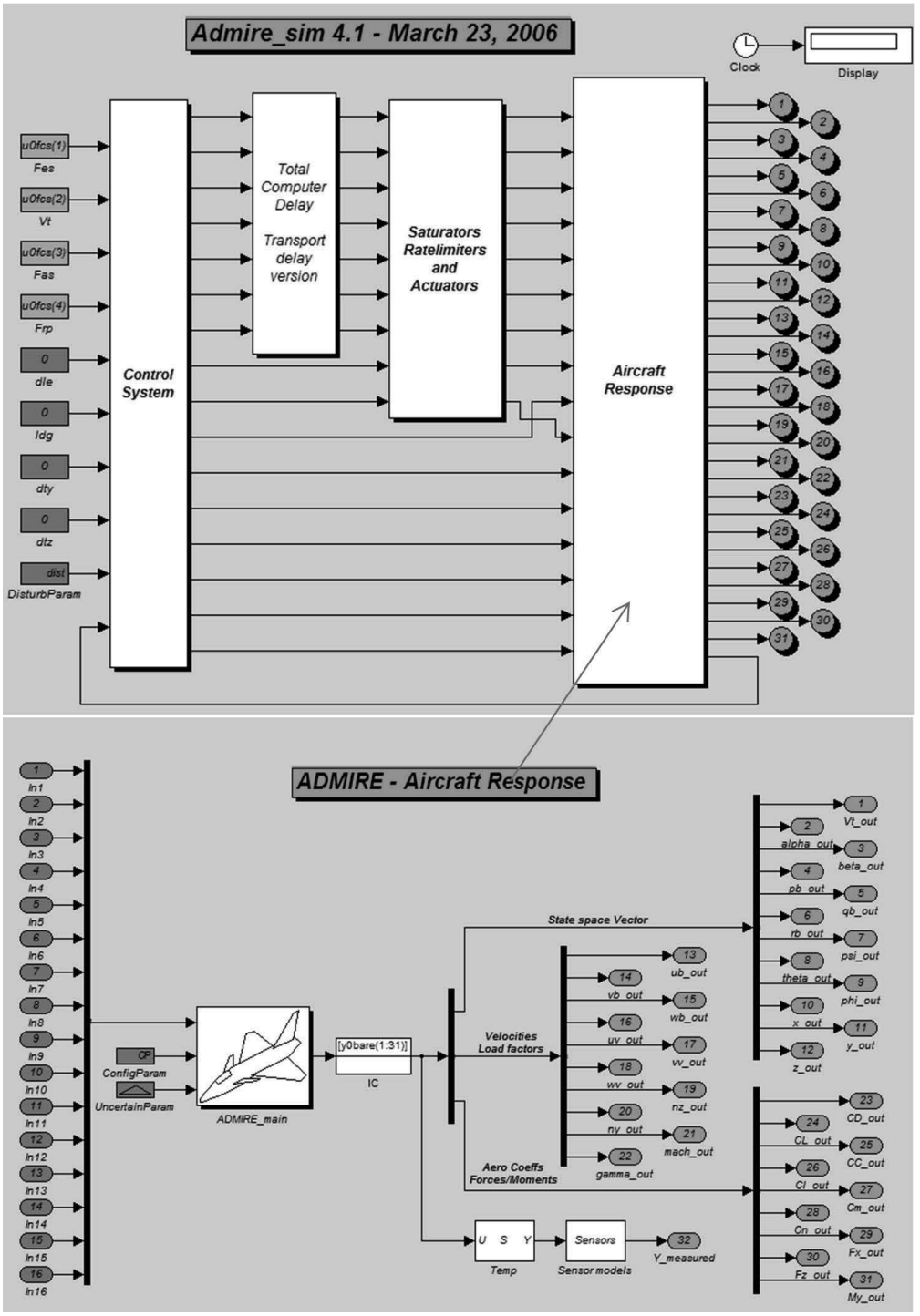

Figure 1. ADMIRE: Main graphical window simulation and aircraft response[11].

https://doi.org/10.1017/S0001924000008575 Published online by Cambridge University Press

Stroe[8] solved the Lurie-Postnikov problem using general vibration equations involving linear transformations. Stroe also analysed a holonomic system with dependent variable equations[9], where the WFM was applied to vibration and stability studies in cases of damped holonomic systems.

The selections of H_∞ weighting functions were presented for practical applications by Jiankun *et al*[10], where the authors showed that an H_∞ weighting function for a single-input single-output system could be obtained by considering it as a series of connections of elementary low-order systems. For a constrained control effort, an explicit weighting function was obtained. They proposed a novel method for the selection of weighting functions in an H_∞ mixed sensitivity design to directly control the percentage overshoot. Real-time experimental results were presented for the roll-angle control of a laboratory scale model of a vertical take-off aircraft[10].

Our analysis of longitudinal and lateral motions using the WFM was performed on the Aero-Data Model In Research Environment model (ADMIRE) developed by the FOI[11], based on the Generic Aerodata Model (GAM) developed by SAAB AB in the framework of the GARTEUR Group[12]. 'The ADMIRE describes a generic small-single seated, single-engine fighter aircraft with a delta-canard configuration, implemented in MATLAB/SIMULINK Release 13'[13, p iii]. The stability domains were determined for each flight case for the given configurations.

This paper is part of a project developed at LARCASE laboratory to perform a more complete analysis of an aircraft in subsonic regime as a design tool, based on geometrical parameters. Three real different configurations were analysed and HIRM model was chosen for its instability well known. The WFM was applied to the original non-linear aerodynamics model implemented in ADMIRE simulation, as well as for the model stabilised with control laws, in order to stabilise its flight.

2.0 THE HIRM: MODEL DESCRIPTION AND ITS IMPLEMENTATION IN ADMIRE SIMULATION

The HIRM (High Incidence Research Model)[1,13,14] of a generic fighter aircraft was used in this study. This aircraft model has an envelope defined by a Mach number between 0·15 and 0·5 and altitude of between 100 and 20,000ft for the following angles: the angle-of-attack α = [–10 to 30] degrees, sideslip angle β = [–10 to 10] degrees, elevon angle δ_e = [–30 to 30] degrees, canard angle δ_c = [–55 to 25] degrees, and rudder angle δ_r = [–30 to 30] degrees.

The aerodynamics coefficients were obtained based on wind tunnel and flight tests for a model '... originally designed to investigate flight at high angles of attack ... but [that] does not include compressibility effects resulting from high subsonic speeds.'[14, p 21]. These coefficients were further implemented in the ADMIRE model using the main graphical window simulation presented in Fig. 1, which also shows the response of the aircraft model. The tests and analyses provided in the GARTEUR program were focused on PIO detection, while this paper evaluates a new method to investigate the model's stability.

'The ADMIRE contains twelve states (V_T, α, β, p_b, q_b, r_b, ψ, θ, φ, x_v, y_v, z_v) plus additional states due to actuators and Flight Control System (FCS). Available control effectors are left- and right canard, leading edge flap, four elevons, rudder and throttle setting. The model is also equipped with thrust vectoring capability and an extendable landing gear. The model is prepared for the use of atmospheric turbulence as external disturbance. The ADMIRE is augmented with an FCS in order to provide stability and sufficient handling qualities within the operational envelope (altitude <6km, Mach < 1·2). The FCS contains a longitudinal and a lateral part. ... The lateral controller enables the pilot to perform roll control where the roll motion is initiated around the velocity

https://doi.org/10.1017/S0001924000008575 Published online by Cambridge University Press

vector of the *a/c*, and angle of sideslip control. Sensor models are incorporated. The 20ms flight computer delay on the actuator inputs that is implemented in other versions of ADMIRE was not used here. The model has the facility to define model uncertainties, but this was not used. ADMIRE is implemented in MATLAB and SIMULINK using a combination of standard SIMULINK blocks and S-functions written in C.'[12, p36].

Figure 1 is a screenshot of the ADMIRE window simulation and it is presented here to understand how this model works. Each block is define on different level and for aircraft response a screen shot was considered necessary, because of the ADMIRE_main block which contains the non-linear coefficients given as tables.

The following table contains a summary of the aircraft geometrical data, along with aircraft mass and mass distribution data[13].

Table 1
Summary of the aircraft geometrical data

Parameters	Numerical values [Units]
wing area S	$45m^2$
wing span b	10m
wing mean aerodynamic chord $\bar{c}$	5·2m
Mass m	9,100kg
x-body axis moment of inertia Ix	$21{,}000kgm^2$
y-body axis moment of inertia Iy	$81{,}000kgm^2$
z-body axis moment of inertia I_z	$101{,}000kgm^2$
xz-body axis product of inertia I_{xz}	$2{,}500kgm^2$
z_{eng}	–0·15m
x_{cg}	$0{\cdot}25\bar{c}$

Let us consider a model defined by a nonlinear autonomous system of equations for the longitudinal motion and for its lateral motion, given below as Equations (1) and (2), respectively[13,14,16].

$$\begin{cases} \dot{V} = -\dfrac{\tilde{q}S}{m}C_D + \dfrac{1}{m}T\mathrm{Cos}\alpha - g\mathrm{Sin}\gamma \\ \dot{\gamma} = \dfrac{\tilde{q}S}{mV}C_L + \dfrac{1}{mV}T\mathrm{Sin}\alpha - m\dfrac{g}{V}\mathrm{Cos}\gamma \\ \dot{q} = \dfrac{1}{I_y}\left[\tilde{q}S\bar{c}C_m + x_{CG}\tilde{q}SC_T + z_eT\right] \\ \dot{\theta} = q \end{cases} \quad \ldots (1)$$

$$\begin{cases} \dot{\beta} = p\alpha - r - \dfrac{\tilde{q}S}{mV}C_y + \dfrac{g}{V}\mathrm{Sin}\phi\mathrm{Cos}\theta \\ \dot{p} = -\dfrac{1}{I_x}\left[\left(I_z - I_y\right)qr + \tilde{q}SbC_l\right] \\ \dot{r} = -\dfrac{1}{I_z}\left[\left(I_y - I_x\right)pq + \tilde{q}S\left(\bar{c}C_n - x_{cg}C_y\right)\right] \\ \dot{\phi} = p \end{cases} \quad \ldots (2)$$

The aerodynamic force and moment coefficients contain degrees of non-linearities, as shown in the next Equation (3). Their values were obtained from the ADMIRE simulation[11]:

https://doi.org/10.1017/S0001924000008575 Published online by Cambridge University Press

$$\begin{cases} C_N = C_{N1}(\alpha) + C_{N2}(\alpha,\delta_e) + C_{N3}(\alpha,\delta_c) + C_{N4}(\alpha,\beta,\delta_e) \\ C_T = C_{T1}(\alpha) + C_{T2}(\alpha,\delta_e) + C_{T3}(\alpha,\delta_c) \\ C_m = C_{m1}(\alpha) + C_{m2}(\alpha,\delta_e) + C_{m3}(\alpha,\delta_c) + C_{m4}(|\alpha|)\dot{\alpha} + C_{m5}(\alpha,\delta_e)q + \\ \qquad + C_{m6}(\alpha,|\beta|,\delta_c) + C_{m7}(\alpha,\delta_a) \\ C_D = C_N \mathrm{Sin}\alpha + C_T \mathrm{Cos}\alpha \\ C_L = C_N \mathrm{Cos}\alpha - C_T \mathrm{Sin}\alpha \end{cases} \quad \ldots(3)$$

$$\begin{cases} C_y = C_{y1}(\alpha,|\beta|) + C_{y2}(\alpha,|\beta|,\delta_r) + C_{y3}(\alpha,\delta_a) + C_{y4}(\alpha)\delta_{ca} + C_{y5}(\alpha,|\beta|)p + C_{y6}(\alpha,|\beta|)r \\ C_l = C_{l1}(\alpha,|\beta|) + C_{l2}(\alpha,|\beta|,\delta_r) + C_{l3}(\alpha,\delta_a) + C_{l4}(\alpha,\delta_c)\delta_{ca} + C_{l5}(\alpha,|\beta|)p + C_{l6}(\alpha,|\beta|)r \\ C_n = C_{n1}(\alpha,|\beta|) + C_{n2}(\alpha,|\beta|,\delta_r) + C_{n3}(\alpha,|\beta|,\delta_a) + C_{n4}(\alpha,\delta_c)\delta_{ca} + C_{n5}(\alpha,|\beta|)p + C_{n6}(\alpha,|\beta|)r \end{cases}$$

3.0 THE WEIGHT FUNCTION METHOD

The main objective of this paper is to study, based on the above Equation (1) and (3), the HIRM stability when the Weight Function Method (WFM) is applied. The WFM is based on the following theorem:

Theorem[9]: Given the autonomous system, $\dot{x} = f(x)$, $x \in R^n$, if $w_k(x_1, x_2 \ldots x_n)$ exists such that $dV = \sum_{k=1}^{n} x_k w_k dx_k$ is a total exact differential, then its stability is given by $W = \sum_{k-1}^{n} x_k w_k f_k$ as follows:

- if W is negative-definite, the solution is asymptotically stable;
- if W is the null function, the solution is neutrally stable; or
- if W is positive-definite, the solution is unstable.

The WFM replaces the classical Lyapunov function by finding a problem with a method which obtains a number of weight functions equal to the number of the first-order differential equations modelling the system[8,9]. The difference between these two methods is that the weight functions method finds one function at a time, with their number equal to the number of the first-order differential equations.

The WFM's basic principle is to find three positive weight functions for a system with four first-order differential equations, where the fourth weight function is a constant, imposed by the author. The total weight function $W = \sum_{k=1}^{4} w_k x_k f_k$ is defined, and its sign should be negative to ensure the stability of the aircraft.

3.1 Longitudinal aircraft model

For longitudinal aircraft modelling, it was assumed that $\gamma = 0$, $V = const$ and $h = const$; with these conditions, the first two equations of Equation (1) become equivalent to:

$$T = mg\,\mathrm{Sin}\alpha + \tilde{q}S\left(C_D \mathrm{Cos}\alpha - C_L \mathrm{Sin}\alpha\right) = mg\,\mathrm{Sin}\alpha + \tilde{q}SC_T \quad \ldots(4)$$

https://doi.org/10.1017/S0001924000008575 Published online by Cambridge University Press

and the longitudinal model is described by:

$$\begin{cases} \dot{\alpha} = q \\ \dot{q} = \dfrac{\tilde{q}S}{I_y}\left[\left(x_{cg}+z_e\right)\left(C_{T1}(\alpha)+C_{T2}(\alpha,\delta_e)+C_{T3}(\alpha,\delta_c)\right)+\dfrac{mg}{\tilde{q}S}z_e\,\mathrm{Sin}\,\alpha\right]+ \\ \quad +\dfrac{\tilde{q}S\bar{c}}{I_y}\left[C_{m1}(\alpha)+C_{m2}(\alpha,\delta_e)+C_{m3}(\alpha,\delta_c)+C_{m4}(|\alpha|)\dot{\alpha}+C_{m5}(\alpha,\delta_c)q+C_{m6}(\alpha,|\beta|,\delta_c)+C_{m7}(\alpha,\delta_a)\right] \end{cases}$$

or

$$\begin{cases} \dot{\alpha} = q \\ \dot{q} = \dfrac{\bar{q}S}{I_y}\left[\bar{c}C_{M1}+\left(x_{cg}+z_e\right)C_T+\dfrac{mg}{\bar{q}S}z_e\,\mathrm{Sin}\,\alpha\right]+\dfrac{\bar{q}S}{I_y}\bar{c}C_{M2}q \end{cases} \quad \ldots (5)$$

where C_{M1} is the sum of C_{m1}, C_{m2}, C_{m3}, C_{m6} and C_{m7}, and $C_{M2} = C_{m4} + C_{m5}$.
The total weight function W_{long} is given by Equation (6), where $f_1 = \alpha, f_2 = \dot{q}$;

$$W_{long} = \sum_{k=1}^{2} w_k x_k f_k = w_{long1}\alpha f_1 + w_{long2} q f_2 = w_{long1}\alpha q + w_{long2} q\left[\frac{\bar{q}S}{I_y}\left(\bar{c}C_{M1}+\left(x_{cg}+z_e\right)C_T+\frac{mg}{\bar{q}S}z_e\,\mathrm{Sin}\,\alpha\right)+\frac{\bar{q}S}{I_y}\bar{c}C_{M2}q\right]$$

$$= \alpha q\left(w_{long1}+w_{long2}\frac{mg}{I_y}z_e\frac{\mathrm{Sin}\alpha}{\alpha}\right)+w_{long2}q\left[\frac{\bar{q}S}{I_y}\left(\bar{c}\left(C_{M1}+C_{M2}q\right)+\left(x_{cg}+z_e\right)C_T\right)\right] \quad \ldots (6)$$

In the first parenthesis of Equation (6) that multiplies the term αq, the first weight function w_{long1} is defined as $w_{long1} = -w_{long2}\dfrac{mg}{I_y}z_e\dfrac{\mathrm{Sin}\alpha}{\alpha} > 0$ for any positive value of w_{long2}, because $z_e = -0{\cdot}15$m is negative from the aircraft geometry, a value implemented in the ADMIRE simulation. The next step consists of replacing w_{long1} in Equation and obtaining the total longitudinal weight function W_{long}, as defined in Equation (7), where its sign depends on the sign of q.

$$W_{long} = w_{long2} q\left[\frac{\bar{q}S}{I_y}\left(\bar{c}\left(C_{M1}+C_{M2}q\right)+\left(x_{cg}+z_e\right)C_T\right)\right] \quad \ldots (7)$$

3.2 Lateral aircraft model

The lateral model was given in Equation (2), and using the following notations: $i_1 = \left(I_z - I_y\right)/I_x$ $i_3 = \left(I_y - I_x\right)/I_z$ Equation (2) is written in the form:

$$\begin{cases} \dot{\beta} = p\alpha - r - \dfrac{\tilde{q}S}{mV}C_y \\ \dot{p} = -i_1 qr + \dfrac{\tilde{q}Sb}{I_x}C_l \\ \dot{r} = -i_3 pq + \dfrac{\tilde{q}S}{I_z}\left[\bar{c}C_n - x_{cg}C_y\right] \\ \dot{\phi} = p \end{cases} \text{ or } \begin{cases} \dot{\beta} = y_\beta\beta + \left(y_p+\alpha\right)p + \left(y_r - 1\right)r + y_{\delta_a}\delta_a + y_{\delta_r}\delta_r \\ \dot{p} = \left(l_\beta + l_{\alpha\beta}\alpha\right)\beta + l_p p + \left(l_r - i_1 q\right)r + l_{\delta_r}\delta_r + \left(l_{\delta_a} + l_{\alpha\delta_a}\alpha\right)\delta_a \\ \dot{r} = n_\beta\beta + \left(n_p + n_{\alpha p}\alpha + i_3 q\right)p + n_r r + n_{\delta_r}\delta_r + \left(n_{\delta_a} + n_{\alpha\delta_a}\alpha\right)\delta_a \\ \dot{\phi} = p \end{cases} \quad \ldots (8)$$

https://doi.org/10.1017/S0001924000008575 Published online by Cambridge University Press

The system of Equations (8) can be simplified as follows:

$$\begin{cases} f_1 = y_\beta \beta + Y_p p + Y_r r + y_{\delta_a}\delta_a + y_{\delta_r}\delta_r \\ f_2 = L_\beta \beta + l_p p + L_r r + l_{\delta_r}\delta_r + L_{\delta_a}\delta_a \\ f_3 = n_\beta \beta + N_p p + n_r r + n_{\delta_r}\delta_r + N_{\delta_a}\delta_a \\ f_4 = p \end{cases} \quad \ldots (9)$$

where $f_1 = \dot{\beta}, f_2 = \dot{p}, f_3 = \dot{r}, f_4 = \dot{\phi}$ and:

$$\begin{aligned} &Y_p = \left(y_p + \alpha\right),\ Y_r = \left(y_r - 1\right) \\ &L_\beta = \left(l_\beta + l_{\alpha\beta}\alpha\right),\ L_r = \left(l_r - i_1 q\right),\ L_{\delta_a} = \left(l_{\delta_a} + l_{\alpha\delta_a}\alpha\right) \\ &N_p = \left(n_p + n_{\alpha p}\alpha + i_3 q\right),\ N_{\delta_a} = \left(n_{\delta_a} + n_{\alpha\delta_a}\alpha\right) \end{aligned} \quad \ldots (10)$$

By denoting the state vector $x_k = [\beta\ p\ r\ \phi]^T$ the lateral weighting function is then given as:

$$\begin{aligned} W_{lat} &= \sum_{k=1}^{4} w_{latk} x_k f_k = w_{lat1}\beta f_1 + w_{lat2} p f_2 + w_{lat3} r f_3 + w_{lat4}\phi f_4 = \\ &= w_{lat1}\beta\left(y_\beta\beta + Y_p p + Y_r r + y_{\delta_a}\delta_a + y_{\delta_r}\delta_r\right) + w_{lat2} p\left(L_\beta\beta + l_p p + L_r r + l_{\delta_r}\delta_r + L_{\delta_a}\delta_a\right) + \\ &+ w_{lat3} r\left(n_\beta\beta + N_p p + n_r r + n_{\delta_r}\delta_r + N_{\delta_a}\delta_a\right) + w_{lat4}\phi p \\ W_{lat} &= \left[w_{lat1}\beta Y_r + w_{lat3}\left(N_p p + n_r r + n_{\delta_r}\delta_r + N_{\delta_a}\delta_a\right)\right] r + \beta\left(w_{lat1} y_\beta \beta + w_{lat3} n_\beta r\right) + \\ &+ w_{lat1}\beta\left(Y_p p + y_{\delta_a}\delta_a + y_{\delta_r}\delta_r\right) + w_{lat2} p\left(L_\beta\beta + l_p p + L_r r + l_{\delta_r}\delta_r + L_{\delta_a}\delta_a\right) + w_{lat4}\phi p \end{aligned} \quad \ldots (11)$$

To solve the stability analysis problem, the first weight function is defined from the third term of the lateral weighting function, Equation (11), where w_{lat3} is a constant defined by the authors as equal to 1 in this paper, so that:

$$w_{lat1} = -w_{lat3}\frac{n_\beta r}{y_\beta \beta} \quad \ldots (12)$$

Equation (12) is replaced in Equation (11), to obtain:

$$\begin{aligned} W_{lat} = &\left[w_{lat3} r\left(N_p - \frac{n_\beta}{y_\beta}Y_p\right) + w_{lat2} l_p p + w_{lat4}\phi\right] p + \\ &+ \left[-w_{lat3}\frac{n_\beta}{y_\beta}\left(Y_r r + y_{\delta_a}\delta_a + y_{\delta_r}\delta_r\right) + w_{lat2} L_r p\right] r + w_{lat2} p\left(L_\beta\beta + l_{\delta_r}\delta_r + L_{\delta_a}\delta_a\right) + w_{lat3}\left(n_r r + n_{\delta_r}\delta_r + N_{\delta_a}\delta_a\right) r \end{aligned} \quad \ldots (13)$$

The second weight function, w_{lat2} , can be defined as a function of the w_{lat3} positive function:

$$w_{lat2} = w_{lat3}\frac{n_\beta}{y_\beta L_r p}\left(Y_r r + y_{\delta_a}\delta_a + y_{\delta_r}\delta_r\right) \quad \ldots (14)$$

The last step in our analysis is to find the total w_{lat} lateral weight function, defined in Equation (15), so that the w_{lat4} function can be given in Equation (16) as a function of w_{lat3}.

https://doi.org/10.1017/S0001924000008575 Published online by Cambridge University Press

$$W_{lat} = \left[w_{lat3} \frac{n_\beta l_p}{y_\beta L_r r} \left(y_{\delta_a} \delta_a + y_{\delta_r} \delta_r \right) + w_{lat4} \phi \right] p + \\ + w_{lat3} \left[\frac{n_\beta}{y_\beta L_r} \left(Y_r + y_{\delta_a} \delta_a + y_{\delta_r} \delta_r \right) \left(L_\beta \beta + l_{\delta_r} \delta_r + L_{\delta_a} \delta_a \right) + \left(n_r r + n_{\delta_r} \delta_r + N_{\delta_a} \delta_a \right) r + N_p r p + \frac{n_\beta}{y_\beta} p \left(\frac{l_p}{L_r r} - Y_p \right) \right] \quad \ldots (15)$$

$$w_{lat4} = -w_{lat3} \frac{n_\beta l_p}{y_\beta L_r r \phi} \left(y_{\delta_a} \delta_a + y_{\delta_r} \delta_r \right) \quad \ldots (16)$$

Finally, the final weight function w_{lat} is determined from w_{lat1}, w_{lat2} and w_{lat4}, given by Equations (12), (14) and (16), and as a function of w_{lat3}.

$$W_{lat} = w_{lat3} \left[\begin{array}{l} \frac{n_\beta}{y_\beta L_r} \left(Y_r + y_{\delta_a} \delta_a + y_{\delta_r} \delta_r \right) \left(L_\beta \beta + l_{\delta_r} \delta_r + L_{\delta_a} \delta_a \right) + \\ \qquad + \left(n_r r + n_{\delta_r} \delta_r + N_{\delta_a} \delta_a + N_p p \right) r + \frac{n_\beta}{y_\beta} p \left(\frac{l_p}{L_r r} - Y_p \right) \end{array} \right] \quad \ldots (17)$$

4.0 RESULTS

The longitudinal motion's results are presented for a range of angles of attack, elevon angles and canard angles defined as $\alpha = [-10 \text{ to } 30]°$, $\delta_e = [-30 \text{ to } 30]°$, $\delta_c = 0°$, and sideslip angle $\beta = 2°$. For the lateral motion, the roll rate $p = [-10 \text{ to } 10]°/s$, the yaw rate $r = [-5 \text{ to } 5]°/s$, the sideslip rate $\beta = [0 \text{ to } 10]°$ and the bank angle $\Phi = [-20 \text{ to } 20]°$.

The system defined by Equation and is linearised about a specific equilibrium point, and the results are presented for longitudinal and lateral motions with and without control laws in Figs 5 and 8, respectively. In this context, investigations based on the HIRM database and using the WFM have shown the stability and instability fields and the simple stable solutions for the different system configurations.

4.1 Longitudinal motion

An analysis of the mathematical model was performed, based on the weight function W_{long1} given by Equation (6) and with w_{long2} positively defined. The results are for a system with a null canard angle, sideslip angle $\beta = 1°$, and for the same variation of angle-of-attack and elevon deflection as presented for the equilibrium solution.

In this case, based on Equation (7), a dependence on the sign of q can be observed. The weight function w_{lon2} is equal to 1, the smallest integer. The variation of the total weight function W versus the angle-of-attack and elevon deflection are given in Fig. 2(a) for negative values, $q = -5°/s$ and in Fig. 2 (b) for positive values, $q = 5°/s$. The sign of q changes when the stability field is unstable, and vice versa. The aircraft is simple stable for the pairs of angle-of-attack and elevator angle given in Fig. 3

The simple stable solution varies between ($\alpha = -10°$, $\delta_e = -14°$) and ($\alpha = 25{\cdot}4°$, $\delta_e = 29{\cdot}93°$), as shown in Fig. 3. The two equilibrium curves for elevon and canard deflection angles versus angle-of-attack are shown in Fig. 4. The symmetrical elevon deflection angle was estimated using Equations (18) and (19):

https://doi.org/10.1017/S0001924000008575 Published online by Cambridge University Press

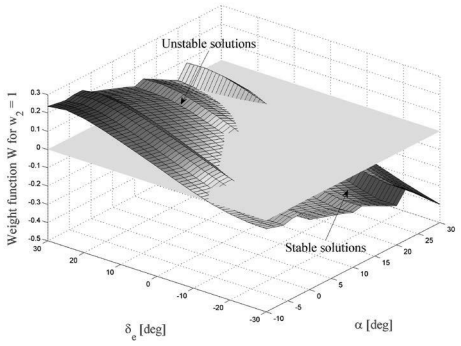

(a)

Figure 2. Total weight function *W* for a complete range angle-of-attack/elevon deflection, with a null canard deflection and negative pitch angle for longitudinal motion.

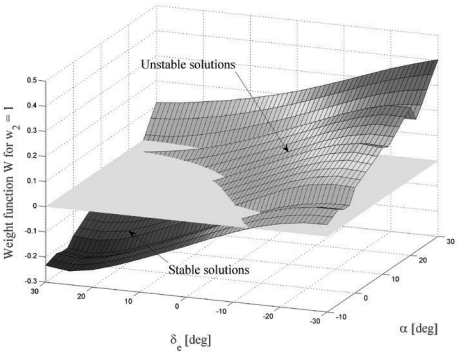

(b)

Figure 3. Total weight function *W* for a complete range angle-of-attack/elevon deflection, with a null canard deflection and positive pitch angle for longitudinal motion.

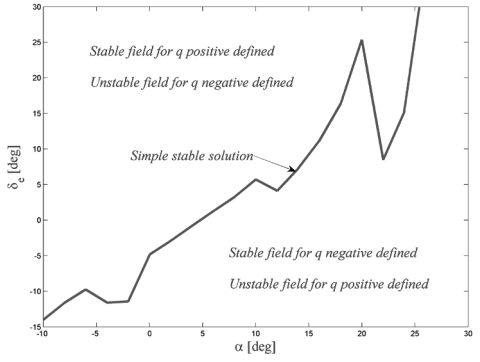

Figure 4. Stability/instability fields for longitudinal motion using the weight function method with w_2 = 1.

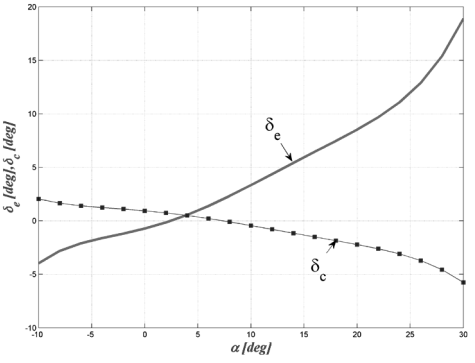

Figure 5. Equilibrium curves for elevon and canard deflection angles versus angle-of-attack.

$$\delta_e = \frac{\delta_{ei} - \delta_{ey}}{2}, \begin{cases} \delta_{ei} = \delta_{lie\_in} + \delta_{rie\_in} \\ \delta_{ey} = \delta_{loe\_in} + \delta_{roe\_in} \end{cases} \quad \ldots (18)$$

where:

$$\begin{aligned} &\delta_{lie\_in} - \text{left outboard elevation angle} \\ &\delta_{rie\_in} - \text{right outboard elevation angle} \\ &\delta_{loe\_in} - \text{left inboard elevation angle} \\ &\delta_{roe\_in} - \text{right inboard elevation angle} \end{aligned} \quad \ldots (19)$$

The total weight function variation with α for the longitudinal motion, for w_{long2} = 1, is given by Equation (7) and is shown in Fig. 5. The smallest integer 1 was used for w_{long2} ,which multiplies a term whose sign is analysed here (w_1), so that for any higher value of the constant w_{long2}, the

https://doi.org/10.1017/S0001924000008575 Published online by Cambridge University Press

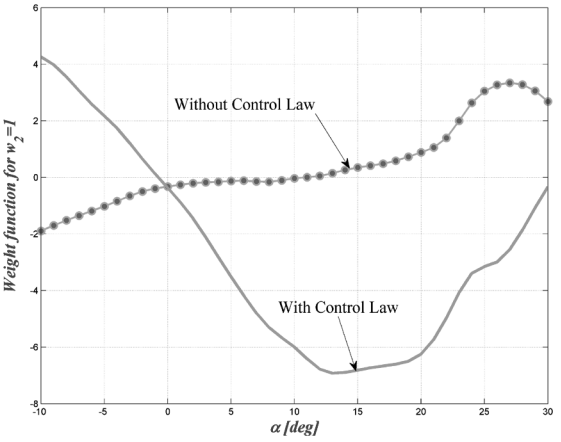

Figure 6. Weight function *W* without/with a control law at equilibrium for longitudinal motion.

variation of *W* is the same only its value increases. The red curve (marker line) shows the variation of the total weight function with α in Fig. 5, where it can be seen that for:

- $\alpha = [-10° \text{ to } 10{\cdot}8776°)$ and $\delta_e = (-4° \text{ to } 3{\cdot}585°)$ the aircraft is asymptotically stable;
- $\alpha = 10{\cdot}8776°$ and $\delta_e = 3{\cdot}585°$ the aircraft is neutrally stable;
- $\alpha = (10{\cdot}8776° \text{ to } 30°]$ and $\delta_e = (3{\cdot}585° \text{ to } 19°)$ the aircraft is unstable;

To stabilise the model, a control law was used for the longitudinal aircraft motion, given by:

$$\delta_e = \delta_{e0} + k_a a + k_q q \qquad \ldots (20)$$

Using this control law with the regulator gains $k_\alpha = 0{\cdot}4$ and $k_q = 1{\cdot}284$, provided by ADMIRE simulation[11], the stability field increases, as shown by the total weight function *W*, represented by the green curve (no marker line) in Fig. 5. In order to analyse aircraft's stability as function of α and δ_e, the value of δ_e at equilibrium corresponding to the angle-of-attack α was obtained from Fig. 4. It was concluded that, with aircraft longitudinal motion, for:

- $\alpha = (-0{\cdot}64° \text{ to } 30°]$ and $\delta_e = (-1{\cdot}063° \text{ to } 26°)$ the aircraft is asymptotically stable;
- $\alpha = -0{\cdot}64°$ and $\delta_e = -1{\cdot}063°$ the aircraft is neutrally stable;
- $\alpha = [-10° \text{ to } -0{\cdot}64°]$ and $\delta_e = (-10° \text{ to } -1{\cdot}063°)$ the aircraft is unstable.

4.2 Lateral motion

Based on the weight functions w_{lat1}, w_{lat2} and w_{lat4} given in Equation (12), (14), (16) and with w_{lat3} positively defined by the authors, results are presented for a sideslip angle $\beta = 2°$, roll rate $p = [-10 \text{ to } 10]°/s$, yaw rate $r = [-5 \text{ to } 5]°/s$, bank angle $\Phi = [-20 \text{ to } 20]°$, and the same variation of angle-of-attack and elevon deflection presented for longitudinal motion in this paper. The sign of Equation (17) depends on the signs of *p*, *r* and ϕ.

The weight function w_{lat3} has the same value as that of the longitudinal motion, the smallest integer equal to 1. This value was chosen because w_{lat3} multiplies a parenthesis, and as could be

https://doi.org/10.1017/S0001924000008575 Published online by Cambridge University Press

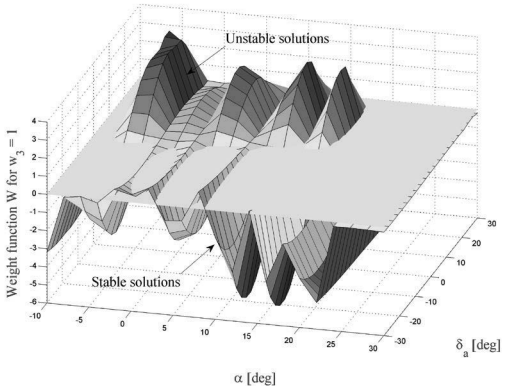

Figure 6(a). Total weight function W for a complete range of angle-of-attack/elevon deflection, for lateral motion.

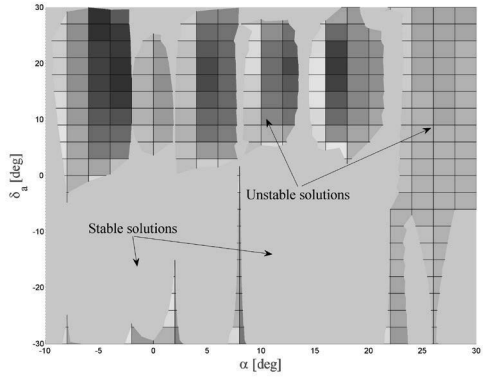

Figure 6(b). Total weight function W for a complete range of angle-of-attack/elevon deflection, for lateral motion.

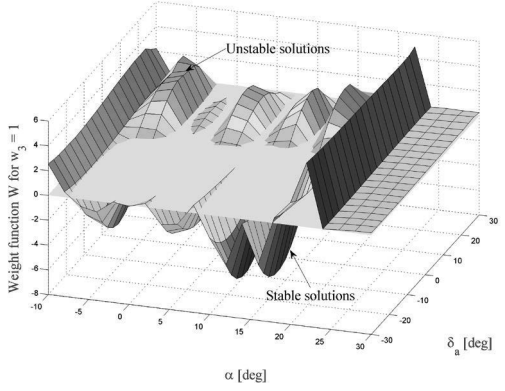

Figure 6(c). Total weight function W for a complete range of angle-of-attack/elevon deflection, for lateral motion.

any value, positive definite, the sign of W function does not change. The variations of the total weight function W versus angle-of-attack and elevon deflection are given in Fig. 6(a) for negative value $p = -10°/s$, $r = -5°/s$, $\Phi = -20°$, (b) for null values $p = 0°/s$, $r = 0°/s$, $\Phi = 0°$ and (c) for positive values $p = 10°/s$, $r = 5°/s$, $\Phi = 20°$). Figure 6 (b) is a section with the plane, i.e. $W = 0$·

https://doi.org/10.1017/S0001924000008575 Published online by Cambridge University Press

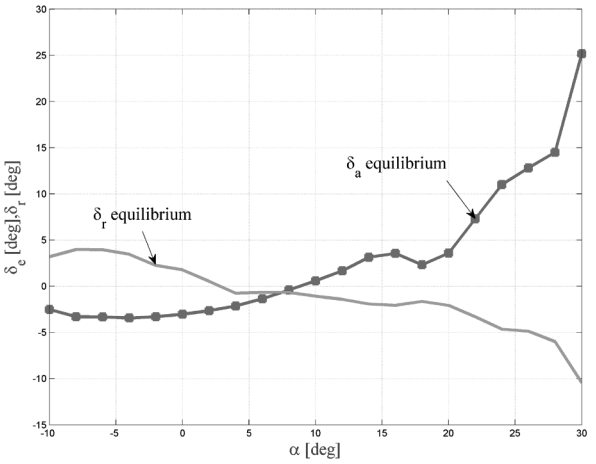

Figure 7. Equilibrium curves for elevon and rudder deflection angles versus angle-of-attack.

It is not easy to detail all the stability/instability fields concerning the lateral motion. Figure 6 (a), (b) and (c) shows the variation of the weight function with angle-of-attack and elevon/rudder deflection.

The two equilibrium curves for elevon and rudder deflection angles versus angle-of-attack are shown in Fig. 7. The asymmetrical elevon deflection angle was estimated based on the notations used in Equation (19):

$$\delta_a = \frac{\delta_{ai} - \delta_{ay}}{2}, \begin{cases} \delta_{ai} = \delta_{lei\_in} - \delta_{rei\_in} \\ \delta_{ay} = \delta_{loe\_in} - \delta_{roe\_in} \end{cases} \quad \ldots (21)$$

The total lateral weight function is given by Equation (17), in which $w_{lat3} = 1$, the smaller integer positive define, and is plotted in Fig. 8 where the red curve (no marker line) represents the solution without a control law, and the stability and instability fields are the following for various values of α and δ_a:

the aircraft is asymptotically stable for

- α = [–10° to –8·046°) and δ_a = (–2·55° to –3·272°);
- α = (4·996° to 8·362° and δ_a = (–1·754° to –0·244°);
- α = (12·29° to 19·389°) and δ_a = (1·924° to 3·201°);
- α = (22·97° to 30°) and δ_a = (9·07° to 25·15°);

the aircraft is simple stable for:

- α = –8·046° and δ_a = –3·272° ;
- α = 4·996° and δ_a = –1·754°/α = 8·362° and δ_a =–0·244°;
- α = 12·29° and δ_a = 1·924°/α = 19·389 and δ_a = 3·201°;
- α = 22·97° and δ_a = 9·07°;

the aircraft is unstable for:

- α = (–8·046° to 4·996°) and δ_a = (–3·272° to –1·754°);
- α = (8·362° to 12·29°) and δ_a = (–0·244° to 1·924°);
- α = (19·3890 to 22·970) and δ_a = (3·2010 to 9·070);

https://doi.org/10.1017/S0001924000008575 Published online by Cambridge University Press

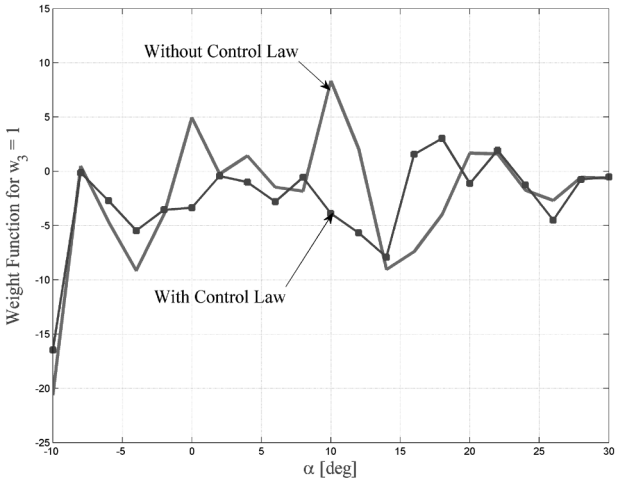

Figure 8. Weight function *W* with and without a control at equilibrium for lateral motion.

A control law was used to stabilise the model, given by:

$$\delta_a = \delta_{a0} + \quad k_p p + k_\phi \phi$$

$$\delta_r = \delta_{r0} + \quad k_\beta \beta + k_{\dot{\beta}} \dot{\beta}$$

This control law was used with the regulator gains given as k_p = 0·52106, k_φ = –0·27704, k_β = 7·6727, and $k_{\beta dot}$ = –4·9301 implemented in ADMIRE simulation[11]; the field of stability increases for the range of angles of attack from –10° to 15·67° (see the blue marker curve in Fig. 8), as shown next for different values of α and δ_a:
asymptotically stable for:

- α = (–10° to 15·67°) and δ_a = (–2·551° to 3·47°)
- α = (19·45° to 20·73°) and δ_a = (3·186° to 4·894°)
- α = (23·21° to 30°) and δ_a = (9·712° to 25·15°);

simple stable for:

- α = 15·67° and δ_a = 3·47°;
- α = 19·45° and δ_a = 3·186°;
- α = 20·73° and δ_a = 4·894°;
- α = 23·31° and δ_a = 9·712°;

unstable for:

- α = (15·67° to 19·45°) and δ_a = (3·47° to 3·186°) ;
- α = (20·73° to 23·21°) and δ_a = (4·894° to 9·712°).

5.0 CONCLUSIONS

The manoeuvrability of an aircraft is determined by its ability to change its attitude and speed about three axes (longitudinal, lateral and vertical). The main aim of this paper was to determine the positive weight functions by using the Weight Function Method to analyse the stability/instability fields of an HIRM model and to stabilise this model using control laws.

https://doi.org/10.1017/S0001924000008575 Published online by Cambridge University Press

For the autonomous system of differential equations used in this paper, the WFM gives the stability and instability fields. Based on the analysis presented above for the nonlinear model, the oscillatory behaviour was observed for the lateral motion, equivalent to an unstable one, and for longitudinal motion it could be seen that the sign of q changes the stability field to unstable and vice versa.

The HIRM is an unstable model and the control law introduced for each motion, longitudinal and lateral, was used to stabilise its flight in the range of $\alpha = (-0{\cdot}64° \text{ to } 30°]$ and $\delta_e = (-1{\cdot}063° \text{ to } 26°)$ for longitudinal motion, and $\alpha = (-10° \text{ to } 15{\cdot}67°)$ and $\delta_a = (-2{\cdot}551° \text{ to } 3{\cdot}47°)$ for lateral motion.

REFERENCES

1. YOICHI, S. and YASUMI, K. Numerical weight function method for structural analysis formulation for two-dimensional elasticity and plate structures, *J Society of Naval Architects of Japan,* 2003, **193**, pp 33–38, ISSN 0514–8499.
2. KIM, J.H. and LEE, S.B. Calculation of stress intensity factor using weight function method for a patched crack with debonding region, *Engineering Fracture Mechanics*, 2000, **67**, pp 303–310.
3. PARIS, P.C., MCMEEKING, R.M. and TADA, H. The weight function method for determining stress intensity factors, cracks and fracture – Proceedings of the Ninth national Symposium on Fracture Mechanics, 1976, 76–1712, pp 471–489.
4. WU, X.R. and CARLSSON, J. The generalised weight function method for crack problems with mixed boundary conditions, *J Mechanics and Physics of solids*, 1983, **31**, (6), pp 485–497.
5. FETT, T. An analysis of the three-point bending bar by use of the weight function method, *Engineering Fracture Mechanics*, 1991, **40**, (3), pp 683-686.
6. SCHNEIDER, G.A. and DANZER, R. Calculation of stress intensity factor of an edge crack in a finite elastic disc using the weight function method, *Engineering Fracture Mechanics*, 1989, **34**, (3), pp 547-552.
7. VAINSHTOK, V.A. and VARFOLOMEYEV, I.V. Application of the weight function method for determining stress intensity factors of semi-elliptical cracks, *Int J Fracture*, 1987, **35**, (3), pp 175-186, DOI: 10.1007/BF00015587.
8. STROE, I. Weight Functions Method in stability study of vibrations, SISOM 2008 and Session of the Commission of Acoustics, Bucharest, Romania, 29–30 May 2008. online < http://www.imsar.ro/SISOM%20&%20ACOUSTICS_%20Papers_%202008/A14.pdf >, verified 29 March 2013.
9. STROE, I. and PARVU, P. Weight functions method in stability study of systems, PAMM, Proc Appl Math Mech, **8**, 10385 – 10386 (2008) / DOI 10.1002/pamm.200810385.
10. JIANKUN, H., BOHN, C. and WU, H.R. Systematic H_∞ weighting function selection and its application to the real–time control of a vertical take–off aircraft, *Control Engineering Practice*, 2000, **8**, pp 241–252.
11. Admirer4p1, http://www.foi.se/en/Our-Knowledge/Aeronautics/Admire/Downloads/, verified 31 March 2013.
12. GARTEUR FM(AG12), PIO Analysis of a Highly Augmented Aircraft, GARTEUR/TP-120-07, 5 September 2001.
13. LARS, F. and ULRIK, N. ADMIRE The Aero-Data Model In a Research Environment Version 4.0, Model Description, FOI-R-1624-SE, ISSN-1650-1942, December 2005.
14. TERLOUW, J.C. *et al* Robust flight control design challenge. Problem formulation and manual: The high incidence research model (HIRM), GARTEUR/FM/AG-08 TP-088-4, 2 February 1996.
15. GARTEUR FM(AG12), PIO Analysis of a Highly Augmented Aircraft, GARTEUR/TP-120-07, 5 September, 2001.
16. SCHMIDT, L.V. *Introduction to Aircraft Flight Dynamics*, *AIAA Education Series*, 1998.